Nanoliposomal Omega-3 Fatty Acids Promote Adult Hippocampal Neurogenesis through the BDNF/TrkB Pathway in C57BL/6 Mice

Foltran RB*[1], Diaz G*[2,3,4], Stefani KM[5], Feliu MS[6], Impa Condori AR[6], Colapietro AA[5], Montagna DR[7], Ambrosi V[2,3,4,8], Godoy MF[6], Guidi SM[2,3,8], Nanni M[9], Diaz SL[7,10]

1 Instituto de Fisiología, Biología Molecular y Neurociencias (IFIBYNE), UBA-CONICET, Buenos Aires, Argentina.

2 Instituto Tecnología de Alimentos, INTA, Buenos Aires, Argentina.

3 Instituto de Ciencia y Tecnología de Sistemas Alimentarios Sustentables (ICyTeSAS) INTA – CONICET, Buenos Aires, Argentina.

4 Facultad de Farmacia y Bioquímica (FFyB), Cátedra de Bromatología, UBA. Buenos Aires, Argentina.

5 Instituto de Biología Celular y Neurociencias (IBCN), UBA-CONICET, Buenos Aires, Argentina.

6 Facultad de Farmacia y Bioquímica (FFyB), Cátedra de Nutrición, UBA. Buenos Aires, Argentina.

7 Instituto de Biociencias, Biotecnología y Biología traslacional (IB3), UBA-CONICET. Buenos Aires, Argentina.

8 Universidad de Moron, Escuela Superior de Ingeniería, Informática y Ciencias Agroalimentarias (ESIICA, UM), Argentina.

9 Universidad Nacional de Hurlingham (UNAHUR), Argentina.

10 Facultad de Farmacia y Bioquímica (FFyB), Cátedra de Técnicas de Bioterio, UBA. Buenos Aires, Argentina.

Abstract

Polyunsaturated fatty acids (PUFAs) are fundamental for different cellular and structural processes, especially regarding the nervous system. However, its incorporation in food has many bioaccessibility limitations, making it important to find new ways of its consumption. In this work, nanoencapsulated PUFAs orally administrated to male mice for 8 weeks showed better bioavailability when compared to administration of free acids, also improving the effects on hippocampal neuronal survival and on the Brain derived neurotrophic factor biological pathway in this region.

This would mean that the form of administration of the fatty acids can alter not only how much and how preserved they reach the central nervous system, but also have a differential impact in the diverse processes they contribute to.

Introduction

Polyunsaturated fatty acids (PUFAs) are indispensable structural and signaling components of cellular architecture. While Saturated Fatty Acids (SFA) and Monounsaturated Fatty Acids (MUFA) serve primarily as oxidative substrates or structural anchors, scientific interest in neurobiology focuses, on omega-3 Polyunsaturated fatty acid (*n*-3 PUFAs), specifically, eicosapentaenoic acid (20:5, *n*-3; EPA) and docosahexaenoic acid (22:6, *n*-3; DHA). These molecules are far more than energy substrates; they are preferentially esterified into neuronal membrane phospholipids. Within this lipid bilayer, their high degree of unsaturation modulates critical physicochemical properties, i.e. membrane fluidity, curvature, and the spatial organization of lipid rafts, essential for neurotransmission and synaptic plasticity (McNamara & Carlson, 2006; Rahim et al., 2025).

The physiological efficacy of n-3 PUFAs is dictated by their transition from the diet to the brain parenchyma, a process restricted by the blood-brain barrier (BBB). This transport is not a matter of simple diffusion; it is a highly regulated kinetic event. Recent evidence identifies the Major Facilitator Superfamily Domain-containing protein 2a (MFSD2A) as the primary transporter for lysophosphatidylcholine-bound DHA, while the Fatty Acid-Binding Protein 5 (*Fabp5*) facilitates the uptake of non-esterified forms (Mitchell et al., 2011; Iwao et al., 2023). This transport mechanism represents the physiological bottleneck that determines the neuroprotective efficacy of lipids.

Furthermore, the modern "Western Diet" has shifted the systemic lipid profile toward a pro-inflammatory state, characterized by an excessive *n*-6/*n*-3 ratio and high SFA intake, which respectively competes with *n*-3 PUFAs for desaturation and elongation pathways, and promote membrane lipid remodeling that limits n-3 PUFA incorporation. (Clemente-Suárez et al., 2023). Conventional n-3 incorporation in food, however, is hindered by the extreme susceptibility of methylene-interrupted double bonds to oxidative stress. The resulting lipid peroxidation products not only diminish biological functionality but can also induce cellular toxicity. Consequently, oxidative stability indices and the atherogenic and thrombogenic indices are useful for assessing the quality of “designer” lipids (Chen & Liu, 2020).

To overcome these bioaccessibility limitations, the use of fermented dairy matrices offers a promising strategy as a carrier for omega-3 fatty acids, owing to their ability to optimize bioactive stability and functionality. This approach not only preserves the structural integrity of these fatty acids but also targets the gut-brain axis by modulating the microbiota, potentially establishing a systemic environment conducive to proliferation within the neurogenic niche (O’Mahony & Clarke, 2017). Furthermore, nanotechnology—specifically through nanoemulsions and encapsulation—has been established as a superior strategy to enhance lipid delivery

(Inapurapu et al., 2020). By protecting PUFAs from gastric degradation and optimizing intestinal micellization, these systems significantly increase the concentration of active fatty acids in target tissues (Yang & Ciftci, 2020).

A central objective of this research is to elucidate how this enhanced delivery impacts adult hippocampal neurogenesis in a murine model. The administration of the bioactive compound was based on the metabolic equivalence of the Recommended Daily Intake (RDI) of 250–500 mg for healthy adults established by international organizations (FAO/WHO Report, 2010), integrated into a fermented dairy matrix to ensure its bioavailability and mimic an optimized human consumption scenario. The dentate gyrus (DG) maintains a neurogenic niche where multipotent stem cells expressing Nestin (Nes) transition into mature, Calbindin-positive (Calb1) functional neurons. This continuum is orchestrated by the Brain-Derived Neurotrophic Factor (BDNF) pathway among other factors. While DHA is known to upregulate Bdnf (Eckert et al., 2011; Suárez Pereira, 2015), the specific molecular mechanisms by which nanoencapsulated n-3 PUFAs (DHA-EPA) modulate the expression of markers of neuronal differentiation during this process remain under-investigated.

Therefore, the present study evaluates the effects of orally administered nanoencapsulated n-3 PUFAs (DHA-EPA), delivered via a fermented yogurt matrix, in male C57BL/6 mice over a chronic period. We hypothesize that this formulation increases systemic bioavailability, BBB transport efficiency, and metabolic incorporation compared to free fatty acids, thereby enhancing neuronal survival in the DG and robustly activating the Bdnf signaling cascade, as evidenced by the modulation of key neurogenic and transport markers.

Materials and Methods

Animals

Studies were performed on 51 male, C57BL/6 elite mice purchased at the Instituto de Medicina Experimental, Academia Nacional de Medicina, Buenos Aires, Argentina. Experiments on animals were conducted according to local regulations and were approved by the Institutional Ethical Committee (ResCD-2022-1246-E-UBA-DCT#FMED). Three-four week-old mice, bred in barrier-conditions to maintain an SPF status, were transported in environmentally controlled conditions to our institute's animal facility. After arrival, mice were housed in 1284L Eurostandard Type II Long (365 mm × 207 mm × 140 mm) Tecniplast microisolator cages with filter tops (five to seven animals per cage), with autoclavated aspen shavings as bedding and tissue paper as nesting material. Mice were maintained under controlled conditions, i.e., 22 ± 2°C room temperature, 40-70% relative humidity, 12–12 h light–dark cycle (lights on at 8 a.m.), pelleted food for rodents (Cooperación) and water ad libitum. Cages were changed twice a week. A period of acclimation of 2 weeks was left before the beginning of experiments, and therefore, mice were 5–6 week-old when treatments began.

Yogurt preparation and administration

Raw Materials and Starter Culture

Yogurt was manufactured using commercial pasteurized cow milk (2% w/v fat; *Mastellone Hnos. S.A., Buenos Aires, Argentina*). A lyophilized Direct Vat Set (DVS) thermophilic starter culture, YoFlex® YG-X16 (comprising Streptococcus thermophilus and Lactobacillus delbrueckii subsp. bulgaricus), was provided by Chr. Hansen (Hørsholm, Denmark). Prior to inoculation, the culture was activated by hydrating 3 g of the lyophilized powder in 1000 mL of milk at 45 °C according to the manufacturer's instructions.

Functional Ingredients and Yogurt Preparation

Omega-3 oil (MEG-3™ 2050EE) was sourced from DSM Nutritional Products. Three distinct treatments were established based on the omega-3 delivery system:

- Control: Yogurt without oil supplementation.
- Free Acids: Yogurt supplemented with bulk omega-3 oil (250 mg / 200 mL milk).
- Nano Acids: Yogurt supplemented with a nanoencapsulated omega-3/soy lecithin formulation (10% w/w load). To achieve an equivalent dose of 250 mg of active omega-3 per 200 mL, 316 mg of the nanostructure (provided by Nanotica Agro SRL via an R&D agreement with INTA) was incorporated.

In both functional formulations, bioactive compounds were homogenized into the milk-sugar base (75 g/L) prior to fermentation.

128 *Yogurt Manufacturing*

129 The mixtures were inoculated with the activated starter culture (2 mL/L) and aseptically
130 distributed into 200 g sterile polypropylene containers. Incubation was performed at 43 ± 1 °C
131 until a target pH of 4.5 was achieved. Samples were then cooled and stored at 4 °C for 28 days
132 for longitudinal analysis.

133 *Yogurt Administration*

134 The different kinds of yogurt were administered to mice by mixing it with a palatable cube. They
135 were made with 10 g of powdered yeast, 66 g of powdered milk, 36 g of sugar, and 14 g of
136 gelatin, for each ice tray (12 cubes) (Foltran et al., 2020). These ingredients were mixed with 2
137 ml of each of the three yogurts and with approximately 60 mL of tap water, forming a thick liquid
138 preparation, which was poured into an ice tray. The 3 cm × 3 cm × 4 cm cubes, weighing around
139 12 g, were kept at 4 °C and were prepared every 6 days. A yogurt containing cube was given per
140 cage, every day between 2 p.m. and 5 p.m. Mice voluntarily ate the cubes, immediately after
141 they were placed in the cages.

142

143 **Experiments:**

144 All mice were divided into 3 groups (control vs the two types of yogurt formulation) for 3
145 different experiments. For the first protocol, 5 mice per group were administered the yogurt
146 cubes for 4 weeks. At the end of the treatment, all mice were deeply anesthetized (20 mg/kg
147 xylazine and 200 mg/kg ketamine) and blood was obtained by intracardiac collection, from
148 which serum was extracted to quantify fatty acids concentrations. After death confirmation,
149 mice were decapitated, brains were removed, and both hippocampus (HC) were obtained,
150 where the left hemi-HCs were prepared for protein extraction and Western blots and the right
151 hemi-HCs were used for mRNA measurements by qRT-PCR.

152 For the second experiment, in order to study neuronal proliferation 18 mice n = 6 per group)
153 were administered yogurt cubes for 4 weeks. The thymidine analog 5-bromo-2'-deoxyuridine
154 (BrdU; Sigma, B9285) was administered to mice at the end of the treatment, in order to label
155 dividing cells. Animals received two ip injections of BrdU, 50 mg/kg each, at a 2 h interval. BrdU
156 was dissolved in 0.9% NaCl at 50 °C. The next day, all mice were deeply anesthetized (20 mg/kg
157 xylazine and 200 mg/kg ketamine) and transcardially perfused with 5 mL of 0.9% NaCl with
158 heparin and 50 mL of 4% paraformaldehyde in 0.1 M phosphate-buffered saline (PBS, pH 7.4)
159 for 15 min. Brains were recovered, post-fixed for 24 h at 4 °C, and cryoprotected with a 30%
160 sucrose solution. Brains were then sliced into 35 µm thick coronal sections through the
161 hippocampus (bregma −0.94 to −3.80) with a freezing microtome. Sections were stored at 4 °C
162 in 0.1 M PBS with 0.1% sodium azide if not used immediately.

163 For the last trial, the yogurt cubes were administered for 8 weeks to 18 mice (6 per group) to
164 study the survival of newborn neurons. Animals received two ip injections of BrdU, 50 mg/kg
165 each, at a 2 h interval for two consecutive days at the end of the 4th week of treatment. Mice
166 were then continued treatment for 4 more weeks, so that BrdU labeled 4 week-old neurons. At
167 the end of the treatment, all mice were deeply anesthetized and transcardially perfused, as
168 stated before.
169
170 **Fatty acid profile determination**
171 Serum fatty acid profile was determined by gas chromatography: Chromatograph: Perkin Elmer
172 Clarus 500; Column: Supelco SP 2560 100 m x 0.25 mm x 0.20 µm; FID detector 280 °C; Carrier
173 gas: helium. Previously, serum lipids were converted into methyl esters according to the Lepage
174 and Roy method as follows: 2 mL of methanol/toluene (4:1) were added to 200 µL of serum,
175 followed by 0.2 mL of acetyl chloride using a vortex mixer. The mixture was incubated at 100 °C
176 for one hour. Then, 5 mL of 6% potassium carbonate was added, and the samples were
177 centrifuged. 1 µL of the toluene layer was injected into the chromatograph. Fatty acid methyl
178 esters (FAMEs) were identified based on their retention times by comparison with the PUFA No.
179 2 (Animal Source) FAME analytical standard (SUPELCO 47015-U). The results (mean ±SD) were
180 expressed as the per cent (%) of total fatty acids content, with a quantification limit of 0.05%
181 (Lepage & Roy, 1986; Rodríguez-Palmero, 1998; Fernandez, 2021).
182
183 **Western Blotting**
184 Tissue was homogenized with 250 µl of RIPA buffer along with protease inhibitors (150 mM NaCl,
185 1% NP-40, 0.5% Sodium deoxycholate, 0.1% SDS, 50 mM Tris) and centrifuged at 4°C for 30 min
186 at 13000 (r/min). The supernatants were recovered and protein levels were quantified by the
187 Bradford protein assay. Samples (50 µgr in 5× loading buffer) were then loaded into SDS-PAGE
188 gels (12 or 15%) and transferred onto nitrocellulose membranes using the Mini-PROTEAN® Tetra
189 System (BIO-RAD) for 1 h.
190 Membranes were incubated for 1 h with blocking solution (5% milk in TBST) and then probed
191 overnight at 4°C with mouse anti-BDNF (1:2000; Icosagen; 327-100 clone 3C11), rabbit anti-p75
192 (1:700; Alomone Labs; ANT-007), rabbit anti-TrkB (1:700; Alomone Labs; ANT-019), and rabbit
193 anti-proBDNF (1:2500; Genocopoeia) in TBST. Actin was used as a loading control (1:2000; Santa
194 Cruz). Binding of primary antibodies was visualized with anti-mouse HRP-conjugated secondary
195 antibody (1:20000; Invitrogen) or anti-rabbit HRP-conjugated secondary antibody (1:20000;
196 Invitrogen). Membranes were developed using the ECL Plus Western blotting substrate (Thermo
197 Fisher Scientific) for chemiluminescence with the Gene Gnome® Imager. Densitometry was

198 carried out using ImageJ software (Schneider et al., 2012). The signal of each protein is expressed
199 after subtraction of background signal and related to actin signal.
200
201 **qRT-PCR**
202 Hippocampal tissue was collected in 250 µL cold Trizol (Invitrogen, Paisley, UK) and
203 homogenized using plastic pestles for homogenizers. RNA was isolated according to the
204 manufacturer's protocol. After addition of chloroform, samples were centrifuged at 11,000 ×g
205 for 15 min at 4 °C. The aqueous phase was transferred and RNA was precipitated with
206 isopropanol, washed with 75% ethanol and resuspended in 15 µL of RNase-free DEPC-treated
207 water. RNA concentration of the tissue was quantified with the Qubit 2.0 Fluorometer (RNA
208 Assay BR Kit, Invitrogen). To ensure genomic DNA removal, 1 µg of total RNA was treated with
209 1 U/µL of DNase I (Invitrogen) for 15 min. RNA purity and absence of residual DNA were verified
210 by qPCR using non-reverse-transcribed RNA as a negative control. Samples were stored at −80
211 °C until further use.
212 Reverse Transcription Quantitative Polymerase Chain Reaction (RT-PCR) was carried out in a
213 StepOnePlus Real-Time PCR System (Applied Biosystems, CA, USA), and the data were analyzed
214 with StepOne software v2.2. The retrotranscription and amplification reactions were performed
215 in a total volume of 10 µl buffer solution containing 2 µl of template RNA, 5 µl of 2× iTaq universal
216 SYBR® Green reaction mix (2x), 0.125 µl iScript reverse transcriptase (Applied Biosystems), 2.08
217 µl RNase-free DEPC-treated water and 0.4 µl of each primer (400 µM). Primers for BDNF (Brain-
218 Derived Neurotrophic Factor), FABP5 (Fatty Acid Binding Protein 5), CALB (Calbindin) and Nest
219 (Nestin) were designed using Primer Express software (Applied Biosystems) and described in
220 table 1.
221 The thermal cycling profile consisted of:
222 -UNG pre-incubation: 50 °C for 2 min.
223 -Initial denaturation: 95 °C for 1 min.
224 -Amplification (40 cycles): 95 °C for 15 s and 60 °C for 1 min.
225 -Melt curve analysis: 95 °C (15 s), 60 °C (1 min), and a final ramp to 95 °C at 0.6 °C/s to confirm
226 amplicon specificity.
227
228 To ensure the robustness of the gene expression analysis, three independent biological
229 replicates were processed per experimental group, following the recommendations of the MIQE
230 guidelines (Bustin et al., 2009). Each biological sample was analyzed in triplicate using qRT-PCR.
231 This balanced design allows for an accurate estimation of experimental error even with

biological sample sizes of n=3, ensuring that the observed differences possess true statistical and biological significance.

Target gene expression was normalized against β-actin (ACTB) as the internal reference gene. The dynamic range was established using a six-point standard curve derived from three independent biological replicates, each processed in technical triplicate (n=9 per dilution). R2 values and amplification efficiencies were calculated based on mean Cq values, incorporating a housekeeping gene (also analyzed in triplicate) for normalization. Relative CT (threshold cycle) values were calculated by subtracting the CT value of the housekeeping gene ACTB (beta-actin) from the CT values. Relative expression was calculated as E^−ΔCt, where E is the efficiency measured for each set of primers.

Gene Symbol	Accession No.	Primer Sequence (5' →3')	E (%)	R^2	Dynamic Range
Actb	NM_007393.5	**F:** ACCAGTTCGCCATGGATGAC **R:** TGCCGGAGCCGTTGTC	97.019	0.995	10^2 - 10^7
Bdnf	NM_001285418.1	**F:** CATAGACAAAAGGCACTGGAACTC **R:** TAAGGGCCCGAACATACGAT	92.000	0.980	10^2 - 10^7
Fabp5	BC002008.1	**F:** CGACAGCTGATGGCAGAAAA **R:** CAGGCCACCGTCTTGGAA	91.788	0.993	10^2 - 10^7
Calb1	NM_009788.4	**F:** GCTCCGCGCACTCTCAA **R:** TGACTGCAGGTGGGATTCTG	98.828	0.940	10^2 - 10^7
Nes	NM_016701.3	**F:** GGTCACTGTCGCCGCTACTC **R:** AAGCGGACGTGGAGCACTA	94.788	0.989	10^2 - 10^7

Table 1. Primer sequences and qPCR performance characteristics.
Accession No. refers to the NCBI GenBank database. $\boldsymbol{E}$ **(%)** represents the amplification efficiency calculated from the slope of the standard curve ($E=[10^{(-1/slope)}-1]\times100$. $\boldsymbol{R}^2$ denotes the coefficient of determination for the linear regression. **Dynamic Range** indicates the interval of template concentration where linearity was maintained. All assays were performed in technical triplicate using SYBR Green chemistry on a StepOnePlus™ Real-Time PCR System.

Immunofluorescence

Newborn cells in the DG were revealed by immunostaining against BrdU as previously published (Diaz et al., 2012). Free-floating sections were exposed to 2 N HCl for 1 h. Sections were then incubated overnight at 4 °C with a mouse anti-BrdU antibody (1:1000; Developmental Studies Hybridoma Bank, concentrated). Nonspecific binding was reduced by 1 h incubation in a saturation solution containing 2 g/L gelatin (Merck) and 0.25% triton in PBS prior to primary antibody incubation. Next day, the tissue was incubated for 2 h with an anti-mouse-A488 (1: 500; Invitrogen). All primary and secondary antibodies were diluted in the saturation solution. Finally, sections were incubated with Hoechst (1: 10000, Invitrogen) to dye the nucleus of cells. The number of BrdU-labeled cells was quantified with a fluorescence microscope (Olympus IX81)

262 with a 20× objective, on serial sections through the entire hippocampus. One out of six series
263 was counted (180 µm intervals, 10 sections per series). BrdU-labeled cells were counted in the
264 sub-granular zone of the granule-cell layer over the entire DG. Cells were considered to be $BrdU^+$
265 when their nuclei were completely filled with fluorescence or showed clear patches of variable
266 intensity (classic dilution pattern for survival assays).
267
268 **Statistical Analysis**
269 Group differences were analyzed using one-way analysis of variance (ANOVA). Assumptions of
270 normality and homogeneity of variances were assessed using the Shapiro–Wilk and Bartlett
271 tests, respectively. When variance heterogeneity was detected, statistical analyses were
272 performed using either Welch's one-way ANOVA or generalized least squares (GLS) models that
273 explicitly accounted for heteroscedasticity. For GLS analyses, models allowing different variance
274 structures were compared to homoscedastic models using likelihood ratio tests, and the final
275 model was selected by balancing goodness-of-fit and parsimony. Post hoc comparisons were
276 performed using Tukey's test following classical ANOVA and GLS models, whereas Games–
277 Howell tests were used following Welch's ANOVA. In fatty acid analyses, p-values were adjusted
278 for multiple testing using the Benjamini–Hochberg false discovery rate (FDR) procedure, applied
279 separately to individual fatty acids and fatty acid classes. Body weight was analyzed using a two-
280 way repeated-measures ANOVA with week as a within-subject factor and treatment as a
281 between-subject factor. Sphericity was assessed using Mauchly's test and Geenhouse-Geisser
282 corrections were applied when necessary. In all analyses, $p < 0.05$ was considered statistically
283 significant, whereas values between 0.05 and 0.1 were considered a trend.
284

285 **Results**

286 *Body weight*

287 Mice were weighed across every week of treatment to control for potential changes due to the
288 different treatments. Analyses showed an interaction between treatment and number of weeks
289 ($p = 0.030$), with no difference in treatment ($p = 0.145$) but significant changes across weeks (p
290 $<.001$). As expected, given their age, all mice gained some weight along the experimental
291 protocol but no differences were revealed between experimental groups.

292

293 *Fatty acids profile*

294 Individual serum levels of the SFA lauric (C12:0), myristic (C14:0) and palmitic (C16:0) were not
295 altered by the treatments, whereas the SFA stearic (C18:0) and lignoceric (C24:0) showed a trend
296 to higher values in the group that consumed the nanoencapsulated version of omega-3 fatty
297 acids in yogurt compared to the control group (Table 1).

298 On the other side, both omega-3–fortified yogurt groups exhibited a trend to lower serum oleic
299 acid (C18:1 n-9) levels compared with the control group, whereas no effect was observed on
300 palmitoleic acid (C16:1 n-7) concentrations (Table 1).

301 Regarding the essential PUFAs linoleic acid (C18:2 n-6) and α-linolenic acid (C18:3 n-3), no
302 significant differences were observed among groups. Likewise, arachidonic acid (C20:4 n-6)
303 levels were not significantly affected by the treatments.

304 Eicosapentaenoic acid (EPA, C20:5 n-3) showed a trend toward higher serum concentrations in
305 the supplemented groups compared with the control (ANOVA $p = 0.07$; FDR-adjusted $p = 0.1633$)
306 (Figure 1.C; Table 1). The control group exhibited intra-group variability, whereas both omega-
307 3-enriched yogurt formulations resulted in more homogeneous and consistently elevated EPA
308 levels. Although these differences did not reach statistical significance after multiple-
309 comparison correction, the observed pattern suggests a potential treatment-related effect on
310 circulating EPA.

311 Docosahexaenoic acid DHA (C22:6 n-3) levels were higher in the free-fatty acid group than in the
312 control group, although the difference was not statistically significant (Figure 1.B). The
313 nanoencapsulated yogurt formulation produced a significant increase in serum DHA levels
314 compared with both control and free-fatty acids groups ($p=0,0000755$). Consequently, the group
315 consuming the nanoencapsulated omega-3 yogurt exhibited a higher total n-3 fatty acid content
316 (Figure 1.A) and a lower n-6/n-3 ratio (Figure 1.D), relative to the other groups . This finding
317 suggests that nanoencapsulation may protect DHA from degradation during storage and
318 digestion, thereby enhancing its stability and facilitating intestinal absorption, as reflected by
319 increased serum DHA levels.

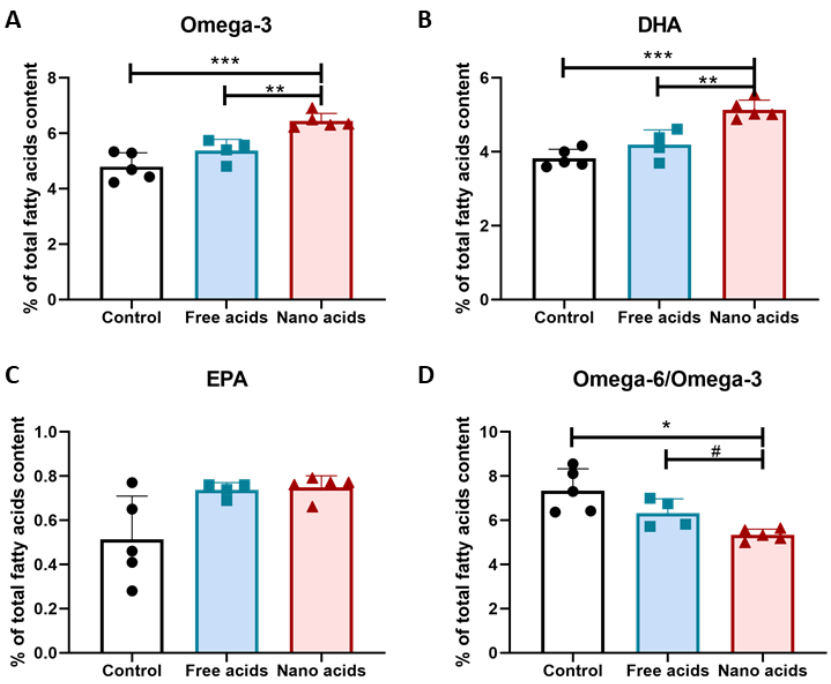

Figure 1. Omega-3 fatty acids profile and n-6/n-3 ratio in serum. Results are expressed as the percentage (%) of total fatty acids content. (A) Total % of fatty acids from the Omega-3 family. (B-C) Individual % for DHA and EPA. (D) Ratio of Omega-6/Omega-3 content in serum. Data are expressed as mean ± SD, n =4-5/group. # 0.05 < p < 0.10; *p < 0.05; **p < 0.01; ***p < 0.001

Serum composition	Control	Free fatty acids	Nano fatty acids	Statistics	P value (FDR)
Lauric acid	0.07 ± 0.023	0.072 ± 0.026	0.052 ± 0.004	F_2 = 2.538	0.2482
Myristic acid	0.316 ± 0.056	0.355 ± 0.066	0.304 ± 0.036	F_2 = 1.1	0.5138
Palmitic acid	18.2 ± 0.765	19.2 ± 1.39	19 ± 1.72	F_2 = 0.713	0.5962
Palmitoleic acid	3.71 ± 0.430	3.66 ± 0.512	3.37 ± 0.414	F_2 = 0.786	0.5962
Stearic acid	8.48 ± 0.287	9.61 ± 0.972	9.46 ± 0.446$^{\#}$	F_2 = 9.025	0.0697
Oleic acid	17.3 ± 1.01	14.7 ± 1.94	14.6 ± 1.39$^{\#}$	F_2 = 5.262	0.0697
Linoleic acid	20.9 ± 1.23	21.6 ± 1.97	21.5 ± 0.632	F_2 = 0.374	0.7495
Alfa-linolenic acid	0.622 ± 0.108	0.598 ± 0.045	0.684 ± 0.084	F_2 = 1.24	0.5138
Arachidonic acid	14 ± 1.72	12.3 ± 1	12.9 ± 2	F_2 = 1.166	0.5138
Lignoceric acid	0.166 ± 0.044	0.205 ± 0.031	0.284 ± 0.078$^{\#}$	F_2 = 5.692	0.0697
EPA	0.514 ± 0.195	0.738 ± 0.033$^{\#}$	0.75 ± 0.052$^{\#}$	F_2 = 3.419	0.1633
DHA	3.83 ± 0.243	4.2 ± 0.395$^{\#}$	5.14 ± 0.262***	F_2 = 25.39	0.00007

Table 2: Fatty acid profile in serum of mice treated with different formulations of yogurt. Results are expressed as the percentage (%) of total fatty acids content. Data are expressed as mean ± SD, n =4-5/group. # 0.05 < p < 0.10; *p < 0.05; **p < 0.01; ***p < 0.001

329

330 *Adult Hippocampal Neurogenesis*

331 In order to analyze if the fatty acid formulation differently altered the process of neurogenesis,
332 BrdU$^+$ cells were quantified by immunohistochemistry in the DG of mice, both at 24 h or 4 weeks
333 after BrdU injection to respectively evaluate the proliferative and survival stages of the
334 neurogenesis process. No significant changes were found in the proliferation of new cells (p =
335 0.67) but it should be noted that inspection of individual data points (Fig. 2A) revealed
336 considerable within-group variability in all the experimental groups. Regarding survival of the
337 newborn cells, we found a tendency to an increase in the mice treated with the
338 nanoencapsulated formulation compared to control (ANOVA p = 0.0921, Post-hoc p =
339 0.0953941) (Fig. 2B).

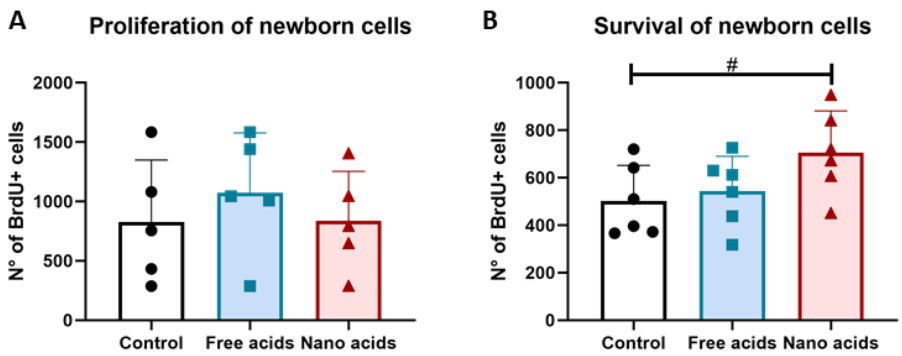

340

341 **Figure 2:** Adult neurogenesis process. (A) Proliferation of new cells in the dentate gyrus (DG) of
342 mice treated with fatty acids supplementation, 24 hs post injection of BrdU. (B) Survival of
343 newborn cells in the DG, 4 weeks post injection of BrdU. Data are expressed as mean ± SD, n
344 =5−6/group. # 0.05 < p < 0.10.

345

346 *RNA analysis*

347 To have an insight into mechanisms behind fatty acid fortification effects in adult neurogenesis,
348 the HC of mice were recovered after the 4 weeks of treatment and RNA expression of different
349 key molecules involved in fatty acid transport, regulation of neurogenesis, and markers of young
350 and mature neurons were analyzed.

351 As stated before, FABP5 plays a role in the uptake, transport, and metabolism of fatty acids, in
352 particular, of DHA. A tendency to a higher FABP5 expression in mice treated with the
353 nanoencapsulated yogurt formulation was detected(ANOVA p = 0.0573, Post hoc p = 0.0993)
354 (Fig. 3A).

355 BDNF has been linked to the regulation of adult hippocampal neurogenesis under diverse
356 conditions, which makes it a big candidate for being involved in the modulation of fatty acids
357 effects in the brain. Indeed, we found a significant increase in BDNF RNA after the treatment (p

358 = 0.000766) (Fig. 3B). Even though the neurotrophin expression levels were enhanced in both
359 yogurt treated groups compared to control (Free-acids p = 0.0006111; Nano-acids p =
360 0.0137006), expression was higher after the free-fatty acids formulation (Free vs Nano p =
361 0.0287450). These results show the same trend observed for the enhancement of the
362 neurogenic process induced by the supplementation with DHA and EPA.
363 Nestin is an intermediate filament protein that identifies neuronal progenitors and young
364 newborn neurons, while Calbindin is a calcium binding protein which serves as a marker of
365 mature, differentiated neurons. As a complementary approach to the immunohistochemistry
366 analysis, and to study the molecular profile of the tissue, we measured RNA expression of both
367 proteins. We found a significant increase in Nestin and Calbindin RNA levels after both fatty acid
368 supplementation treatments (ANOVA Nes p = 0.000271, Calb p = 0.000575). For Nestin, the free-
369 fatty acid formulation showed a higher expression (p = 0.0067782) (Fig. 3C) than the
370 nanoencapsulated acids formulation, whereas for Calbindin levels, they were more enhanced in
371 the nanoencapsulated group (p = 0.0097060) (Fig. 3D). The increased expression of both
372 neuronal markers are in line with the proneurogenic effect of EPA-DHA chronic administration
373 revealed by immunohistochemistry.

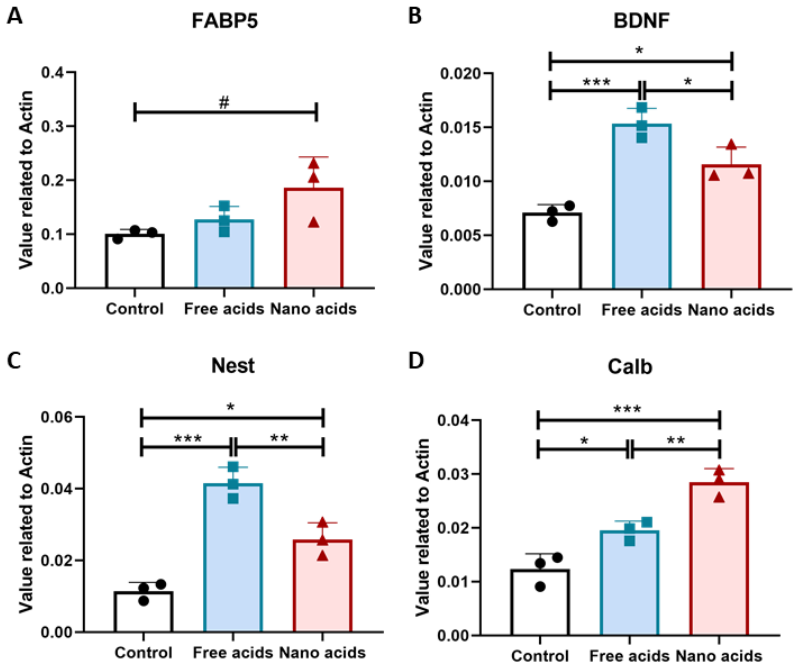

374

375 **Figure 3:** RTqPCRs. RNA was extracted from the HC of mice from the different groups to analyze
376 the transcription levels of (A) FABP5, (B) BDNF, (C) Nestin and (D) Calbindin. Data are expressed
377 as mean ± SD, n =3/group. # 0.05 < p < 0.10; *p < 0.05; **p < 0.01; ***p < 0.001

378

379 *BDNF Pathway*

380 To deepen the understanding of the changes produced in the BDNF pathway, which has a very
381 complex regulation, protein-expression of both BDNF isoforms and their receptors was analyzed
382 in the HC of yogurt-treated mice. Regarding the survival pathway, a significant increase was
383 observed in mBDNF levels (ANOVA p = 0.000191) only in the animals treated with the
384 nanoencapsulated yogurt formulation compared to controls (p = 0.0006301) (Fig. 4A, F),
385 whereas changes in the TrkB receptor between the treated groups and the control mice were
386 not significant (p = 0.4678826) (Fig. 4B, E). On the other hand, for the apoptotic pathway, no
387 significant changes were found for proBDNF (p = 0.2076) though inspection of individual data
388 points revealed considerable within-group variability in the free fatty acids group (Fig. 4C, F). In
389 addition, a tendency towards a decrease in the p75 receptor was observed in mice treated with
390 the free- fatty acid yogurt (ANOVA p = 0.0568, Ctrl vs Free p = 0.0969230) (Fig. 4D, F), which
391 would mean less activation of the cell death mechanisms. Results show that the
392 nanoencapsulated formulation promotes the modulation of the neurotrophin towards the
393 survival pathway, which is in accordance to the other outcomes.
394

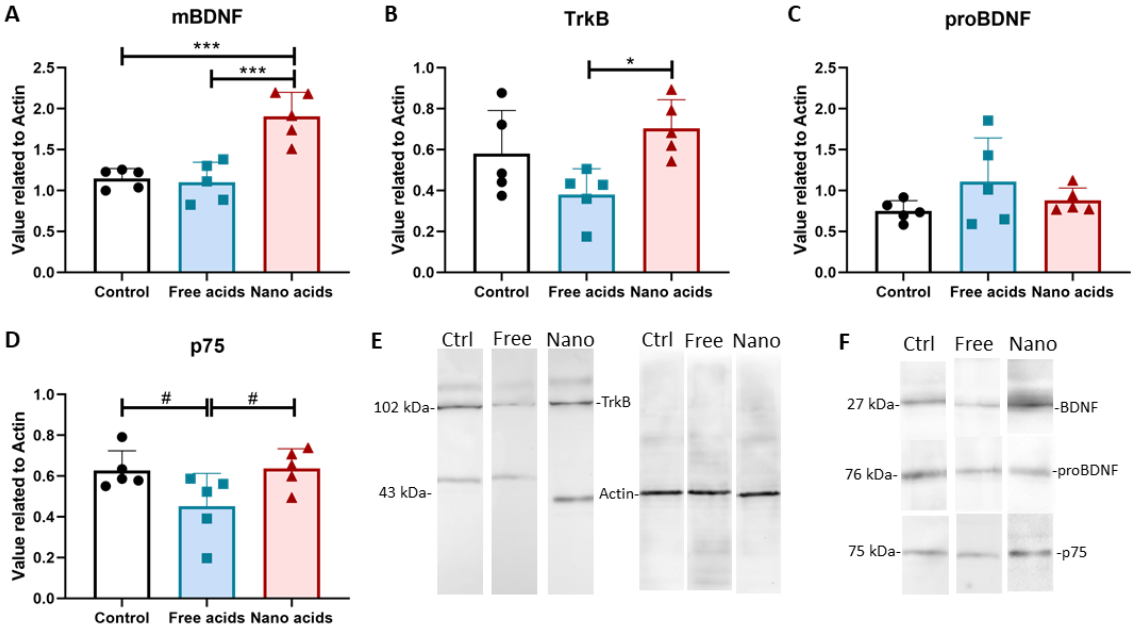

395

396 **Figure 4:** Protein expression of molecules from the BDNF signaling pathway determined by
397 Western Blot and representative membranes. (A)mBDNF. (B)TrkB. (C)proBDNF. (D)p75 for
398 yogurt treated mice after 4 weeks. (E–F) Representative membranes showing signals for TrkB,
399 mBDNF, pro-BDNF, and p75 in Control and fatty acids-treated mice. Data are expressed as mean
400 ± SD, n =5−6/group. # 0.05 < p < 0.10; *p < 0.05; **p < 0.01; ***p < 0.001.
401

Paradigm of assay	Parameter measured	Statistical test	Comparison	Statistics	P value	Figure
Body weight	Body weight	Two-way repeated measures ANOVA	Treatment	$F_{2,48}$ = 2.01	0.145	
			Week	$F_{3.12,149.77}$ = 620.92	<.001	
			Treat:Week	$F_{6.24,149.77}$ = 2.38	0.03	
Fatty acids profile	% of total Omega 3	One way ANOVA	Treatment	F_2 = 21.43	0.00016	**1A**
Fatty acids profile	% of DHA	One way ANOVA	Treatment	F_2 = 25.39	0.00007	**1B**
Fatty acids profile	% of DHA	Tukey post-test	Ctrl - Free		0.19728	
			Ctrl - Nano		0.00007	
			Free - Nano		0.00175	
Fatty acids profile	% of EPA	One way ANOVA	Treatment	F_2 = 3.419	0.1633	**1C**
Fatty acids profile	Omega6/Omega 3 ratio	One way ANOVA	Treatment	F_2 = 11.564	0.01103	**1D**
Fatty acids profile	Omega6/Omega 3 ratio	Tukey post-test	Ctrl - Free		0.214	
			Ctrl - Nano		0.019	
			Free - Nano		0.097	
Proliferation of new cells	N° of BrdU+ cells	One way ANOVA	Treatment	F_2 = 0.414	0.67	**2A**
Survival of newborn cells	N° of BrdU+ cells	One way ANOVA	Treatment	F_2 = 2.807	0.0921	**2B**
Survival of newborn cells	N° of BrdU+ cells	Tukey post-test	Ctrl - Free		0.88569	
			Ctrl - Nano		0.09539	
			Free - Nano		0.21169	
qRT-PCR	Fabp5 signal relative to actin	One way ANOVA	Treatment	F_2 = 4.781	0.0573	**3A**
qRT-PCR	Fabp5 signal relative to actin	Tukey post-test	Ctrl - Free		0.2399	
			Ctrl - Nano		0.0993	

			Free - Nano		0.2932	
qRT-PCR	BDNF signal relative to actin	One way ANOVA	Treatment	F_2 = 29.79	0.00077	**3B**
qRT-PCR	BDNF signal relative to actin	Tukey post-test	Ctrl - Free		0.00061	
			Ctrl - Nano		0.0137	
			Free - Nano		0.02874	
qRT-PCR	Nestin signal relative to actin	One way ANOVA	Treatment	F_2 = 43.37	0.00027	**3C**
qRT-PCR	Nestin signal relative to actin	Tukey post-test	Ctrl - Free		0.00021	
			Ctrl - Nano		0.01023	
			Free - Nano		0.00678	
qRT-PCR	Calbindin signal relative to actin	One way ANOVA	Treatment	F_2 = 33.09	0.00057	**3D**
qRT-PCR	Calbindin signal relative to actin	Tukey post-test	Ctrl - Free		0.02599	
			Ctrl - Nano		0.00046	
			Free - Nano		0.00971	
Western blot	mBDNF signal relative to actin	One way ANOVA	Treatment	F_2 = 19	0.00019	**4A**
Western blot	mBDNF signal relative to actin	Tukey post-test	Ctrl - Free		0.94531	
			Ctrl - Nano		0.00063	
			Free - Nano		0.00037	
Western blot	TrkB signal relative to actin	One way ANOVA	Treatment	F_2 = 5.04	0.0258	**4B**
Western blot	TrkB signal relative to actin	Tukey post-test	Ctrl - Free		0.17166	
			Ctrl - Nano		0.46788	
			Free - Nano		0.02127	
Western blot	proBDNF signal relative to actin	One way ANOVA	Treatment	F_2 = 1.797	0.2076	**4C**
Western blot	P75 signal relative to actin	One way ANOVA	Treatment	F_2 = 3.678	0.0568	**4D**
Western blot	P75 signal relative to actin	Tukey post-test	Ctrl - Free		0.09692	
			Ctrl - Nano		0.99148	
			Free - Nano		0.07893	

402 **Table 3:** P values and statistical information of all procedures performed.

403 **Discussion**

404 The results presented herein demonstrate that chronic administration of nanoencapsulated
405 PUFAs to adult mice, increases the bioavailability of DHA that in turns may promote the survival
406 of the newborn neurons in the HC by enhancing the pro-neurogenic elements of the BDNF
407 pathway. Organoleptic characteristics of the PUFAs-enriched fish diet may prevent people from
408 consuming it regularly. Furthermore, supplementation of fatty acids presents technical
409 difficulties given that, due to their high unsaturation levels, they are unstable and highly
410 susceptible to lipid peroxidation, compromising both their chemical stability and biological
411 functionality. In our study, we took profit of nanotechnology as an alternative delivery system
412 to increase the stability of lipophilic components. Indeed, in vitro studies have demonstrated
413 increased digestibility and bioaccessibility of n-3 PUFAs when administered in nanoemulsions
414 (Yang & Ciftci, 2020; Zhou et al., 2024). We first prepared the nanoformulation of PUFAs using
415 yogurt as a matrix and then mix with other ingredients to form palatable cubes that mice ate
416 voluntarily. Although PUFAs quantities ingested by different animals may have varied depending
417 on the amount of cube ingested, a significant increase in plasma levels of DHA and EPA was
418 measured in both groups administered with the PUFAs for 4 weeks compared to the control
419 group. Remarkably, the concentration of omega-3 family was higher in mice receiving nano acids
420 than those under free acids administration, whereas a lower n-6/n-3 ratio was observed in the
421 group of mice receiving the nanoencapsulated acids. Positive correlations between plasma and
422 brain levels of DHA were already described (Hashimoto 2002; Orchard et al., 2018). Therefore,
423 we could assume that the observed higher plasmatic levels of PUFAs may have a correlate in the
424 brain of treated mice. Indeed, since PUFA are synthesized in small quantities in the brain, the
425 mechanisms by which these fatty acids are transported across the blood-brain barrier are crucial
426 (see rev. in Chouinard-Watkins et al., 2018). In the present study, the FABP-5, a key regulator of
427 DHA uptake in the brain, showed a trend to increase only in the group that received the
428 nanoencapsulated PUFAs. As this group showed the higher plasmatic levels of DHA, this result
429 could altogether show a better bioavailability and distribution of Omega-3 fatty acids under the
430 new formulation. In an elegant series of studies, Pan et al. demonstrated up-regulated
431 expression of brain microvascular FABP5 protein associated with increased brain DHA levels in
432 adult mice fed with a DHA-enriched diet for 21 days (Pan Y, Morris ER, Scanlon MJ, Marriott PJ,
433 Porter CJH, Nicolazzo JA. Dietary docosahexaenoic acid supplementation enhances expression
434 of fatty acid-binding protein 5 at the blood-brain barrier and brain docosahexaenoic acid levels.
435 J Neurochem. 2018 Jul;146(2):186-197). Later they reported that mice knock-out for the Fabp5
436 gene exhibited impaired performances in memory tasks, associated with a reduction in
437 endogenous brain DHA levels (Pan Y, Short JL, Choy KHC, Zeng AX, Marriott PJ, Owada Y, Scanlon

438 MJ, Porter CJH, and Nicolazzo JA. Fatty Acid-Binding Protein 5 at the Blood–Brain Barrier
439 Regulates Endogenous Brain Docosahexaenoic Acid Levels and Cognitive Function. J Neurosci
440 2016; 36(46): 11755-67). These results, together with ours support the hypothesis that
441 increased plasmatic DHA promotes the expression of FABP-5 in the brain, facilitating in turn the
442 increase of DHA levels in the brain.
443 DHA has been inversely associated with cognitive decline in clinics (Mallick et al., 2019). Indeed,
444 populations with a high consumption of fatty fish or fatty acid supplements display lower
445 incidence of neurodegenerative diseases compared to those consuming diets poor in these
446 nutrients (Kalmijn et al., 2004). The process of neurogenesis offers a promising avenue in the
447 search for therapies for aging and neurodegenerative diseases, either by replacing lost neurons
448 or by enhancing brain plasticity. The generation of newborn neurons is well characterized in the
449 adult hippocampus, particularly in the DG, where several factors like neurotrophines, have been
450 shown to facilitate the proliferation and/or survival of newborn neurons (see rev in Balu & Lucki,
451 2009). We were not able to see changes in the proliferation rate of DG neurons in adult mice
452 receiving PUFAs, but mice treated with the nanoencapsulated n-3 Omega fatty acids displayed
453 an increase in the survival of 4-week old neurons, compared with the control group. The
454 enlarged neurogenesis was accompanied by a significant increase of immature and mature
455 markers of neuronal differentiation like Nestin and Calbindin, respectively. Expression of both
456 markers was also enhanced in mice receiving the free acids, revealing that, globally, the n-3
457 omega fatty acids appear to act at different stages of the neurogenic process, i.e, differentiation,
458 and survival of newborn neurons. Increased neuron survival has been already shown in a model
459 of strong deficit of PUFA where rats fed a fish-oil deficient diet for three generations were then,
460 supplemented with DHA for 7 weeks (Kawakita et al., 2006). Another report from rats fed a DHA
461 and EPA-enriched diet during 4 weeks revealed an increase in hippocampal levels of the BDNF
462 as measured by ELISA (Wu et al., 2004). Similar results were observed for BDNF mRNA and
463 protein levels in a transgenic mice model of Alzheimer's disease after 2 months of a DHA-
464 enriched diet (Che et al., 2018) and in C57BL/6 mice chronically supplemented with
465 lysophosphatidylcholine-DHA or -EPA (Sugasini et al., 2017; Yalagala et al., 2019). Our results
466 shed light on these reports describing plastic effects of PUFAs in rodents, as we were able to go
467 deep in the analysis of the BDNF biological pathway. The BDNF is synthesized as a pro-protein,
468 the 32 kDa pro-BDNF that may be cleaved to yield the 13.2-15.9 kDa mature BDNF (mBDNF).
469 The pro-BDNF can release mBDNF after cleavage either intra- or extra-cellularly, or be secreted
470 as pro-BDNF without further modifications. By binding to TrkB receptors, the mBDNF facilitates
471 pro-neurogenic effects, whereas the pro-BDNF may bind different receptors, being the most
472 known the p75, through which pro-apoptotic actions are promoted (see a rev. in Foltran & Diaz,

2016). In this study, increased levels of total BDNF mRNA were detected in both groups of mice that received the n-3 omega fatty acids compared to the control groups. However, when the level of proteins were analyzed, mice receiving the free fatty acids showed a sort of activation of the BDNF pro-apoptotic cascade, with a tendency towards higher levels of the p-75 receptor and something similar for pro-BDNF compared to the other experimental groups. In this line, a previous study in a mice model of Alzheimer disease found that the administration of a DHA/EPA-enriched diet for 2 months decreased the expression of pro-apoptosis factors like Bcl2, Caspase 3 and Caspase 9 (Che et al., 2018). On the contrary, the proneurogenic elements of this biological pathway, like mBDNF and its receptor TrkB, were significantly increased after chronic administration of nanoencapsulated PUFAs, in synthon with the increased survival of the newborn neurons detected in the DG.

Conclusions

In this work, nanoencapsulated PUFAs orally administrated to male mice for 4 or 8 weeks showed better bioavailability when compared to administration of free acids, and this potentially due to an increase of the specific transporter, the FABP-5 specifically in the HC. Furthermore, the nanoformulation enhanced the survival of the DG newborn neurons, possibly in response to an improved proneurogenic balance of BDNF actions. These positive effects can be key to facilitating memory processes or also, to preventing cognitive decline that can occur at advanced ages.

References

- **Chen, J., & Liu, H. (2020).** Nutritional indices for assessing fatty acids: A mini-review. *International Journal of Molecular Sciences*, 21(16), 5695.
- **Clemente-Suárez, V. J., et al. (2023).** Global impacts of western diet and its effects on metabolism and health: A narrative review. *Nutrients*, 15(12), 2749.
- **Eckert, G. P., et al. (2011).** Liposome-incorporated DHA increases neuronal survival by enhancing non-amyloidogenic APP processing. *Biochimica et Biophysica Acta (BBA)-Biomembranes*, 1808(1), 236-243.

- **EFSA Panel on Dietetic Products, Nutrition and Allergies** (NDA). (2012). Scientific Opinion on the Tolerable Upper Intake Level of eicosapentaenoic acid (EPA), docosahexaenoic acid (DHA) and docosapentaenoic acid (DPA). EFSA Journal, 10(7), 2815.
- **Food and Agriculture Organization [FAO]. (2010).** Fats and fatty acids in human nutrition: Report of an expert consultation. FAO Food and Nutrition Paper, 91, 1-166.
- **García-Ortega, A., & Santos-Zea, L. (2020).** Milk proteins as encapsulation systems for lipid-soluble bioactives: A review of recent advances. Journal of Dairy Science, 103(11), 9751-9768. doi.org
- **Inapurapu, S. P., et al. (2020).** Development and characterization of ω-3 fatty acid nanoemulsions with improved physicochemical stability and bioaccessibility. *Colloids and Surfaces A: Physicochemical and Engineering Aspects*, 606, 125515.
- **Iwao, K., et al. (2023).** MFSD2A and FABP5 in the blood-brain barrier: Implications for DHA transport. *Journal of Lipid Research*.
- **Kolanootu, V., & Jayaprakasha, H. M. (2022).** *Influence of fermentation on the stability and bioaccessibility of omega-3 fatty acids in functional dairy beverages*. *LWT - Food Science and Technology, 154*, 112-124. doi.org
- **McNamara, R. K., & Carlson, S. E. (2006).** Role of omega-3 fatty acids in brain development and function: Potential implications for the pathogenesis and prevention of psychopathology. *Prostaglandins, Leukotrienes and Essential Fatty Acids*, 75(4-5), 329-349.
- **Mitchell, R. W., et al. (2011).** Fatty acid transport protein expression in human brain and potential role in fatty acid transport across human brain microvessel endothelial cells. *Journal of Neurochemistry*, 117(4), 735-746.
- **O'Mahony, S. M., & Clarke, G. (2017).** *Nutrition, the gut microbiome and the naturally occurring neurogenesis: A review*. *Molecular Nutrition & Food Research, 61*(1), 1600720. doi.org

- **O'Mahony, S. M., & Clarke, G. (2017).** *Nutrition, the gut microbiome and the naturally occurring neurogenesis: A review*. *Molecular Nutrition & Food Research, 61*(1), 1600720. doi.org

- **Rahim, M. A., et al. (2025).** A Comprehensive Review on Nutritional Traits, Extraction Methods, Oxidative Stability, Encapsulation Technologies, Food Applications and Health Benefits of Omega Fatty Acids. *Food Science & Nutrition*, 13(10), e71008.
- **Su, H. M. (2010).** Mechanisms of n-3 fatty acid-mediated development and maintenance of learning memory performance. *The Journal of Nutritional Biochemistry*, 21(5), 364-373.

- **Suárez Pereira, I. (2015).** *Papel de la neurogénesis hipocampal adulta en los procesos cognitivos que dependen del hipocampo* (Doctoral dissertation, Universidad Pablo de Olavide).
- **Yang, X., & Ciftci, O. N. (2020).** Bioaccessibility of omega-3 fatty acids delivered in nanoemulsions. *Food & Function*, 11, 25-32.
- FAO/WHO Report. Joint FAO/WHO Expert Consultation on the Risks and Benefits of Fish Consumption; FAO Fisheries and Aquaculture Report. No. 979; Rome, 25–29 January 2010.
- McNamara RK, Carlson SE. Role of omega-3 fatty acids in brain development and function: potential implications for the pathogenesis and prevention of psychopathology. Prostaglandins Leukot Essent Fatty Acids 2006; 75: 329-349.
- Chouinard-Watkins R, Scott Lacombe RJ Bazinet RP. Mechanisms regulating brain docosahexaenoic acid uptake: what is the recent evidence? Curr Opin Clin Nutr Metab Care 2018; 21(2): 71-77.
- Iwao T, Takata F, Matsumoto J, Aridome H, Yasunaga M, Yokoya M, Kataoka Y, Dohgu S. Aging decreases docosahexaenoic acid transport across the blood-brain barrier in C57BL/6J mice. PLoS One. 2023 Feb 16;18(2):e0281946
- Pan Y, Scanlon MJ, Owada Y, Yamamoto Y, Porter CJH, and Nicolazzo JA. Fatty Acid-Binding Protein 5 Facilitates the Blood−Brain Barrier transport of Docosahexaenoic Acid. Molecular Pharmaceutics 2015; 12, 4375-85.
- Mallick et al., 2019, Int J Dev Neurosci doi: 10.1016/j.ijdevneu.2019.10.004
- Kalmijn S, van Boxtel MPJ, Ocke M, Verschuren WMM, Kromhout D, Launer LJ. Dietary intake of fatty acids and fish in relation to cognitive performance at middle age. Neurology 2004; 62: 275-80.
- Yang, J.; Ciftci, O.N. In vitro bioaccessibility of fish oil-loaded hollow solid lipid micro-and nanoparticles. Food Funct. 2020, 11, 8637–8647.
- Zhou Q, Lane K, Li W; Evaluating the Stability and Digestibility of Long-Chain Omega-3 Algal Oil Nanoemulsions Prepared with Lecithin and Tween 40 Emulsifiers Using an In Vitro Digestion Model; Foods 2024, 13(15):2407.
- Balu DT & Lucki I. Adult hippocampal neurogenesis: regulation, functional implications, and contribution to disease pathology. Neurosci Biobehav Rev 2009, 33(3):232-52.
- Kawakita E, Hashimoto M & Shido O. Docosahexaenoic acid promotes neurogenesis in vitro and in vivo. Neuroscience 2006; 139: 991-997.

576 • Wu A, Ying Z & Gomez-Pinilla F. Dietary omega-3 fatty acids normalize BDNF levels,
577 reduce oxidative damage, and counteract learning disability after traumatic brain injury in rats.
578 Journal of Neurotrauma 2004; 21(10): 1457-67.
579 • Che H, Zhou M, Zhang T, Zhang L, Ding L, Yanagita T, Xu J, Xue C & Wang Y. Comparative
580 study of the effects of phosphatidylcholine rich in DHA and EPA on Alzheimer's disease and the
581 possible mechanisms in CHO-APP/PS1 cells and SAMP8 mice. Food Function 2018, 9(1):643-54.
582 • Sugasini D, Thomas R, Yalagala PCR, Tai LM & Subbaiah PV. Dietary docosahexaenoic
583 acid (DHA) as lysophosphatidylcholine, but not as free acid, enriches brain DHA and improves
584 memory in adult mice. Scientific Report 2017; 7:11263
585 • Yalagala PCR, Sugasini D, Dasarathi S, Pahan K & Subbaiah PV. Dietary
586 lysophosphatidylcholine-EPA enriches both EPA and DHA in the brain: potential treatment for
587 depression. Journal of Lipid Research 2019; 60:566-78